Lappeenranta-Lahti University of Technology LUT
School of Engineering Science
Computational Engineering and Technical Physics
Technical Physics

Lassi Lehtisyrjä

MEASUREMENT OF GALVANOMAGNETIC PHENOMENA USING PULSED MAGNETIC FIELD SYSTEM

Bachelor's Thesis

Examiner: Professor Erkki Lähderanta

Supervisor: Professor Erkki Lähderanta

ABSTRACT

Lappeenranta-Lahti University of Technology LUT
School of Engineering Science
Computational Engineering and Technical Physics
Technical Physics

Lassi Lehtisyrjä

MEASUREMENT OF GALVANOMAGNETIC PHENOMENA USING PULSED MAGNETIC FIELD SYSTEM

Bachelor's Thesis

2019

36 pages, 15 figures, 4 tables.

Examiner: Professor Erkki Lähderanta

Keywords: pulsed magnetic field, measurement, Hall effect, anomalous Hall effect, magnetoresistance, Shubnikov-de Haas effect, spintronics, semiconductors

In this thesis the pulsed magnetic field system located at the Physics Laboratory at Lappeenranta University of Technology is introduced.

The pulsed magnetic field system (PMFS) is used to measure various galvanomagnetic phenomena in samples, which are typically experimental semiconductor materials or topological structures of the former.

The physical phenomena present in the measurements from the PMFS include the Hall effect, the anomalous Hall effect, magnetoresistance and Shubnikov-de Haas effect. Data from the measurement of the materials resistivity and Hall voltage as a function of temperature and magnetic field can be used to determine many important material characteristics, such as Hall constant, charge carrier density, polarity, mobility and effective mass and the shape of the materials Fermi surface.

Knowledge of these material characteristics are important in the fields of semiconductor research, spintronics (electronics based on the electron spin and its magnetic moment) and quantum computing.

TIIVISTELMÄ

Lappeenrannan-Lahden teknillinen yliopisto LUT
School of Engineering Science
Laskennallinen tekniikka ja analytiikka
Teknillinen fysiikka

Lassi Lehtisyrjä

GALVANOMAGNEETTISTEN ILMIÖIDEN MITTAUS PULSSIMAGNEETTIKENTTÄJÄRJESTELMÄLLÄ

Kandidaatintyö

2019

36 sivua, 15 kuvaa, 4 taulukkoa.

Tarkastaja: Professori Erkki Lähderanta

Hakusanat: pulssimagneettikenttä, mittaus, Hall-ilmiö, anomalinen Hall-ilmiö, Shubnikov-de Haas -ilmiö, spintroniikka, puolijohteet
Keywords: pulsed magnetic field, measurement, Hall effect, anomalous Hall effect, magnetoresistance, Shubnikov-de Haas effect, spintronics, semiconductors

Tässä kandidaatintyössä esitellään Lappeenrannan teknillisen yliopiston fysiikan laboratoriossa sijaitseva pulssimagneettijärjestelmä.

Pulssimagneettijärjestelmällä (PMFS) mitataan lukuisia galvanomagneettisia ilmiöitä näytteissä, jotka tyyppillisesti ovat kokeellisia puolijohdemateriaaleja tai niiden topologisia rakenteita.

Mittausdatassa näkyviä fysikaalisia ilmiöitä ovat mm. Hall-ilmiö, anomalinen Hall-ilmiö, magnetoresistanssi ja Shubnikov-de Haas -ilmiö. Mittausdataa materiaalien resistiivisyydestä ja Hall-jännitteestä lämpötilan ja magneettikentän funktiona voidaan käyttää useiden tärkeiden materiaalisuureiden määrittämiseen, kuten Hall-vakio, varauksenkuljetta-

jien tiheys, polariteetti, mobiliteetti ja efektiivinen massa ja materiaalin Fermi-pinnan muoto.

Näiden materiaaliominaisuuksien tieto on tärkeää puolijohteiden tutkimuksessa, spintroniikassa (elektroniikka, joka pohjautuu elektronin spiniin ja sen magneettiseen momenttiin) ja kvanttitietojenkäsittelyssä.

CONTENTS

LIST OF SYMBOLS AND ABBREVIATIONS

$\mathbf{F}$	Lorentz force
q	Charge of a particle
$\mathbf{E}$	Electric field
$\mathbf{v}$	Particle velocity
$\mathbf{B}$	Magnetic field
R_H	Hall coefficient
E_y	Electric field induced by Hall effect in the y-direction
j_x	Current density in the x-direction
B_z	Magnetic field in the z-direction
j	Current density of charge carriers
n	Charge carrier density
q	Charge carrier charge
v	Drift velocity
E_H	Hall effect electric field
ρ_{xy}	Hall conductivity in the xy-plane
μ_0	Vaccuum permeability
R_A	Anomalous Hall coefficient
M_z	Magnetization in the z-direction
E	Landau energy
ν	An integer
$\hbar$	Reduced Planck's constant $\hbar = \frac{h}{2\pi}$
ω_c	Cyclotron frequency
m^*	Charge carrier effective mass
k_z	Wave number of the charge carrier in the z-direction
I	Bias current through sample
l	Distance between sense contacts
V_σ	Voltage between contacts
A	Cross-sectional area of sample

DMS	Diluted magnetic semiconductor
LUT	Lappeenranta University of Technology
MR	Magnetoresistance
PMFS	Pulsed magnetic field system
SdH	Shubnikov-de Haas
TTL	Transistor-transistor logic

1 INTRODUCTION

1.1 Background

Pulsed magnetic fields have a huge range of possible applications, ranging from materials science and semiconductor development to biology and physiology. As do the applications, so do the parameters of the pulsed fields vary largely, depending on the application. For example, lower energy fields can be used to study effects on biological systems or human physiology [1], while higher energy fields can be used to study effects in bulk steel structures [2].

Situated at Lappeenranta University of Technology (LUT) Physics Laboratory, the pulsed magnetic field system (PMFS) was designed and built to investigate galvanomagnetic properties of solids in pulsed magnetic fields up to 40 Tesla in temperatures ranging from 1.6 to 350 Kelvin. Knowledge of materials magnetic and conductive properties (such as their Hall constant, resistivity as a function of temperature and magnetic field and the properties of their charge carriers) in certain environmental parameters are important in the fields of spintronics, quantum computing and super- and semiconductor research.

The high energies present in such large magnetic fields make for special requirements in the design and construction of the measurement system and the necessary electrical circuits. Also operator safety has to be taken into account.

The PMFS was constructed in 2008 as a collaboration of Ioffe institute and LUT. The objectives for the PMFS were to be used in the research of narrow and zero gap semiconductors, semi-metals, different kinds of homo- and heterostructures and devices, fullerens and superconductors. The ability to also rotate the sample in the magnetic field with high accuracy allows investigating the anisotropy of galvanomagnetic properties of materials and structures.

The PMFS can also be equipped with a compact hydrostatic high pressure cell to measure materials under high hydrostatic pressure and high magnetic field. This is applicable for investigation of energy band structure or other fundamental properties of new compounds.

All previous measurements can also be made with illuminated samples, by adding a light emitting diode to the apparatus or feeding the light in through an optical fiber.

1.2 Objectives and delimitations

The objective of this thesis is to introduce the reader to the working principle of the PMFS and the science which can be done with the instrument. In this thesis the basic physical phenomena present in the measurement, the construction of the apparatus, practicalities of measurement, analysis of the measurement data and implications from the data are explored.

1.3 Structure of the thesis

In the first chapter the underlying physical phenomena are explained. Next the PMFS is introduced and its working principles and components explained. In the the third chapter the typical samples and the practicalities of taking measurements with the system is explored. In the final chapter typical measurement results are exhibited and their meaning in the context of broader research explained.

2 THE PHYSICAL PHENOMENA AT WORK

2.1 Hall effect

The dominating effect observed in the measurements made with the PMFS is the Hall effect.

When an electrical conductor with current flowing through it has a magnetic field applied to it, a voltage is produced, perpendicular to the current and the magnetic field. The effect was discovered by Edwin Hall in 1879 [3].

The effect is created from the nature of electrical current in a conductor. Electrical current is the flow of charge carriers, charged particles (Electrons, holes, ions or all three) along the conductor. A moving, electrically charged particle in a magnetic field experiences a force, the Lorentz force, which is defined by the equation

$$\mathbf{F} = q(\mathbf{E} + \mathbf{v} \times \mathbf{B}) \tag{1}$$

where $\mathbf{F}$ is the Lorentz force, q is the charge of the particle, $\mathbf{E}$ the electric field, $\mathbf{v}$ the velocity of the particle and $\mathbf{B}$ the magnetic field [4].

When no external magnetic field is present, the charge carriers move in approximately straight lines, therefore the density of the charges in the conducting material is uniform and no voltage is created. When external magnetic field is applied the path of the charges is curved perpendicular to both the velocity of the particles and the magnetic field due to the Lorentz force, causing the charges to accumulate on one side of the conductor and therefore creating a voltage difference. Demonstration of this can be seen in Figure 1.

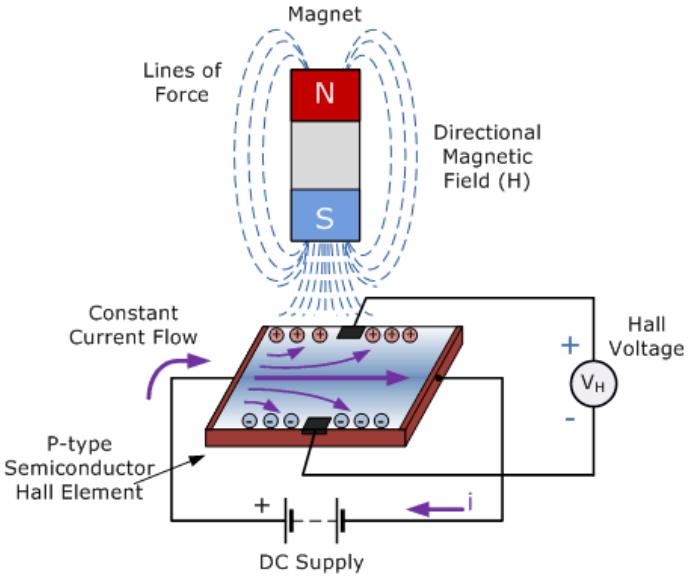

Figure 1. Demonstration of Hall effect in P-type semiconductor [5].

The main quantity describing the strength of the effect in a material is the Hall coefficient. It is defined as

$$R_H = \frac{E_y}{j_x B_z} \tag{2}$$

where E_y is the electric field induced in the y-direction, j_x is the current density of the charge carriers in the x-direction and B_z is the magnetic filed in the z-direction, assuming the current density and magnetic field are perpendicular. Since current density is defined as $j = nqv$, where n is the charge carrier density, q is the charge carrier charge and v is the drift velocity and the electric field caused by the Hall effect $E_H = vB$, the Hall coefficient can be also written $R_H = \frac{1}{nq}$. Therefore it's possible to determine the charge carrier density of a material by measuring its Hall coefficient [6].

The Hall effect has numerous applications, such as magnetometers (Used to measure the strength of magnetic fields). In the field of materials study, the main importance of measuring the Hall voltage is to determine the density of charge carriers and their polarity in the material, which is a crucial quantity in determining many other qualities of the material, such as the electron mobility and drift velocity.

2.2 Anomalous Hall effect

In 1881, Hall discovered that the effect was much larger in ferromagnetic conductors [7]. The equations behind conventional Hall effect do not take in to account the possibility of magnetic order in the conductor.

The empirical relation of Hall conductivity is defined as

$$\rho_{xy} = R_H B_z + \mu_0 R_A M_z \tag{3}$$

where ρ_{xy} is the Hall conductivity in the xy-plane, R_H the conventional Hall coefficient, μ_0 the vacuum permeability, R_A the anomalous Hall coefficient and M_z the magnetization of the conductor in the z-direction. The equation was found to be applicable to many materials over a broad range of external magnetic fields. The anomalous Hall coefficient depends on a number of material specific parameters and the ambient temperature [8].

The mechanisms behind anomalous Hall effect have proven to be complicated and still lack complete understanding today. Three main contributing mechanisms have been identified and they are present in different magnitudes depending on the material and temperature of the measurement: Intrinsic deflection, side jump and skew scattering [9].

The intrinsic deflection is named so as theory predicts its existence in a perfect crystal. When an electric field is applied to the material, electrons gain additional group velocity which is perpendicular to the electric field. This anomalous velocity acts in opposite directions for electrons with different spins and so in ferromagnets, where there is a imbalance of spins, this contributes to the Hall conductivity.

The side jump mechanism is based upon on the same effect that causes intrinsic deflection, but is linked to impurities in the material. Near an impurity in the lattice an electron experiences the electric field from the impurity and causes a deflection to the anomalous velocity described above, therefore contributing to the Hall conductivity.

The skew scattering mechanism is caused by asymmetric scattering of the electrons from an impurity due to spin-orbit coupling and is predicted to dominate the anomalous Hall coefficient in high conductivity ferromagnets.

2.3 Magnetoresistance

Magnetoresistance (MR) is the change of resistivity in a material depending on the magnetic field applied. MR can be caused by many different mechanisms, classical or quantum mechanical, depending on the material or the geometry of the conductor or semiconductor in question. See [10] for further detail. MR can be either positive or negative, meaning that the resistivity of the material either increases or decreases when a magnetic field is applied.

The simplest method of MR is ordinary MR, which is caused by the Lorentz force and is the same in principle as Hall effect. Because the path of the charge carriers curve or become circular (cyclotron orbits) in the magnetic field, their flow through the conductor is impeded. All non-ferromagnetic metals and semiconductors exhibit positive MR.

More complex contributions to positive MR arise from many different phenomena, semiclassical, quantum mechanical or topological, for example.

MR can also have a dependence on the angle between the electrical current and the applied magnetic field in certain materials or topologies, named therefore anisotropic MR. One physical origin of the anisotropicity is attributed to a larger probability of electron scattering in the direction of the magnetic field. The electron cloud of each nucleus deforms slightly as the direction of the magnetization rotates and this deformation changes the amount of scattering by the conduction electrons in the lattice.

Negative MR is a complex subject and is dependent on many different parameters of the material or the topology in question. Especially large negative MR is unusual and therefore an indication of peculiar physics. Negative MR can be explained with quantum mechanics, by for example spin dependent scattering of charge carriers, depending on the material or topology in question. Such effects occur in for example magnetically inhomogeneous material when the material contains ferromagnetic regions, where the magnetic moment is misaligned, causing scattering of the conduction electrons [11].

2.4 Shubnikov-de Haas effect

Shubnikov-de Haas (SdH) effect is the oscillation of the magnetoresistance caused by changing charge carrier density of states at the Fermi energy level in high intensity magnetic fields and low temperatures. The effect is visible only in these conditions, as in

higher temperatures the oscillations are masked by thermal excitations between the Landau levels.

At these low temperatures and intense magnetic fields, the electrons of a metal, semimetal or semiconductor will behave like simple harmonic oscillators. When the magnetic field strength is changed, the frequency of the harmonic oscillators changes proportionally. The resulting energy spectrum is made up of quantized Landau levels separated by the cyclotron energy. These Landau levels are further split by the Zeeman energy. In each Landau level the cyclotron and Zeeman energies and the number of electron states all increase linearly with increasing magnetic field. As the magnetic field increases, the energy of the Landau levels surpass the Fermi energy sequentially, allowing more electron states in the conduction band and the periodic variation of the density of states at the Fermi energy level causes the oscillation of the conductivity as a function of the applied magnetic field [12]. Demonstration of the oscillations can be seen in Figure 2, where the resistance of a sample is plotted as a function of magnetic flux density.

The quantization of the Landau levels in a magnetic field is described by the equation

$$E = (\nu + \frac{1}{2})\hbar\omega_c + \frac{\hbar^2 k_z^2}{2m^*} \tag{4}$$

where ν is an integer, $\hbar$ is the reduced Planck's constant, $\omega_c = qB/m^*$ is the cyclotron frequency, m^* is the charge carrier effective mass and $\hbar k_z$ the component of the momentum parallel to the external magnetic field.

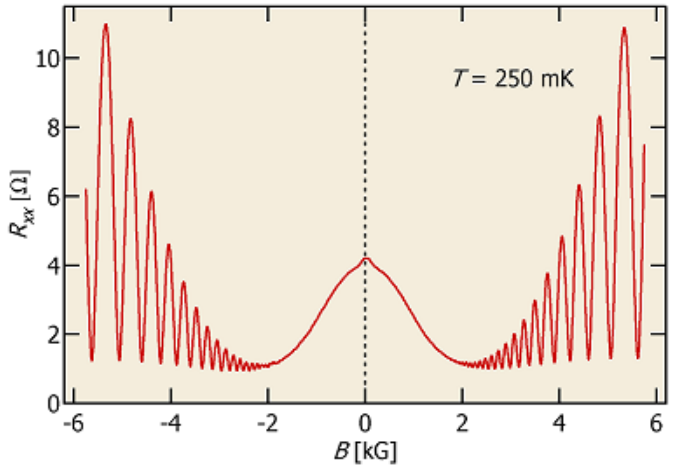

Figure 2. Typical form of SdH oscillations [13].

By exploiting the SdH effect the effective mass of the charge carriers in the material can be obtained from the dependence of the amplitude of the SdH oscillations on temperature in different magnetic fields with a slope proportional to the effective mass [14] therefore allowing the identification of majority and minority charge carrier populations. The oscillations can also be used to determine the Fermi surface of the electrons in the sample from the period of the oscillation in different applied magnetic field directions. Therefore the SdH effect allows the effective study of the energy band structure of the material.

3 THE PULSED MAGNETIC FIELD SYSTEM (PMFS)

The main operating principle of the PMFS is charging up a capacitor bank to high voltages and then discharging the capacitors through a liquid nitrogen immersed multi turn solenoid coil. The sample under test is situated inside the solenoid in a temperature controlled cryostat. Data on the Hall voltage across the sample and resistivity along the sample is captured during the magnetic field pulse, along with parameters of the pulse, such as duration, magnetic field magnitude and temperature of the sample. Main technical parameters of the PMFS can be seen in Table 1.

Table 1. Operational parameters of the PMFS.

Amplitude of the magnetic field	Up to 40 T
Maximum pulse current	5 kA
Maximum pulse duration	11 ms
Temperature range of the sample	1.6 - 350 K
Sample DC bias current	1 μA - 200 mA
Range of measured sample resistances	0.0 1Ω - 100k Ω
Data acquisition	4 channels, 256 Kbyte memory each
Digital-to-analog converters	16 bit, 1 MS/s

The apparatus is situated in its own magnetically shielded room (Figure 3) and is equipped with multiple safety interlocks. The high voltage circuits are fully galvanically isolated from the control room for operator safety. Upon opening the room door interlocks short out the capacitor bank to ground through a discharge resistor and isolate the high voltage transformer from the mains electricity to minimize the risk of electrocution to the operator.

Figure 3. The apparatus in the measurement room. Note the magnetic shielding on the walls.

3.1 Pulse solenoid

The pulse solenoid consists of a copper coil wound with flat wire in a specific geometry, to provide as close to a homogeneous field as possible inside the solenoid. The coil is electrically isolated using a glass fibre and Stycast 2850FT epoxy compound. The solenoid is strengthened with a covering of Hyperten 2000HP epoxy compound and finally clamped together with nonmagnetic bolts and glass fibre laminated end plates. The solenoid can be seen in Figure 4 and it's electrical specifications in Table 2.

The conductor in the solenoid coil is copper, as superconductors cannot be used in such intense magnetic field. This causes some challenges in using the PMFS as the coil heats up considerably due to its non-zero resistance, especially in the higher amplitude pulses.

The solenoid is made specially without using ferromagnetic or conductive materials in the core. This improves the homogeneity of the magnetic field inside the solenoid (Reduction of stray magnetic fields caused by eddy currents in conductive materials) and decreases the noise level (From hysteresis caused by ferromagnetic materials).

The solenoid has been experimentally characterized to confirm the linearity of the magnetic field strength as a function of the current flowing through the coil and to measure

the homogeneity of the magnetic field inside the coil. Because the solenoid has a finite length, the magnetic field inside the solenoid cannot be completely homogeneous. Radially the non-homogeneity of the magnetic field for 7 mm is $\leq$0.09 % and axially for 10 mm $\leq$0.37 % and for 5 mm $\leq$0.09 %

Table 2. Electrical specifications of the pulse solenoid.

Inner diameter	12 mm
Conductor	Flat copper
Inductance	2.377 mH
Resistance	83.05 mΩ
Capacitance	6 μF

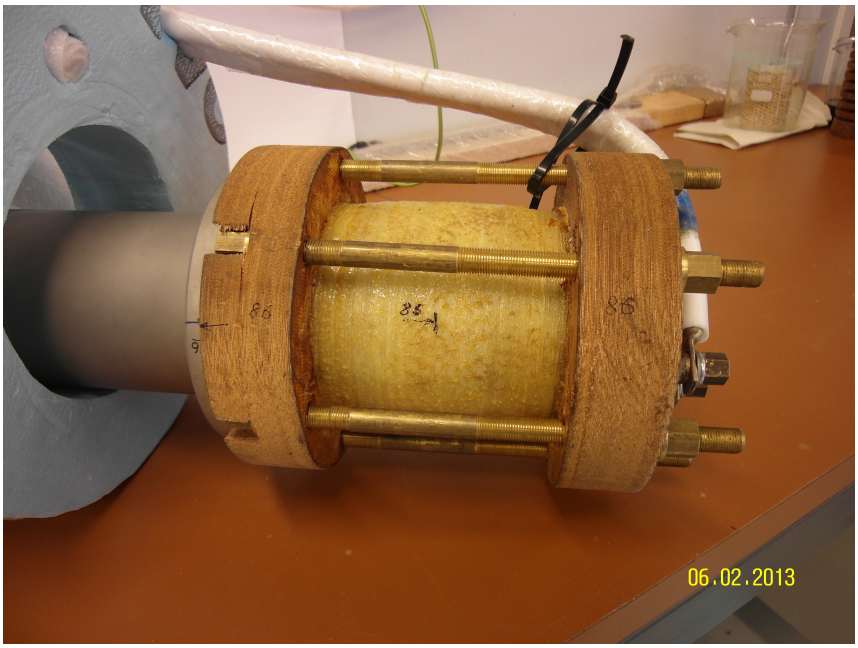

Figure 4. The pulse solenoid attached to the end of the internal cryostat.

3.2 Cryostat and vacuum system

The cryostat is used to cool the solenoid and the sample into the desired temperature and maintain it constant. The pulse solenoid is cooled with liquid nitrogen to decrease the resistance of the coil and dissipate the heat caused by the immense pulse current. Despite this cooling, after maximum amplitude pulse the coil needs to cool down for 30 minutes.

The cryostat is in two parts, external and internal. The external one, insulated with polystyrene foam, houses the solenoid and insulates the liquid nitrogen used to cool the solenoid. The internal vacuum-insulated cryostat houses the sample holder. The sample is housed in a finger protruding from the internal cryostat.

The internal cryostat can also withstand vacuum pressure. With vacuum, the temperature of the sample can be decreased even further. When using liquid helium to cool the sample, the vacuum system also condenses evaporated liquid helium and recycles it back into the cryostat. Pressure meters monitor the pressure of the cryostat and can therefore determine the temperature of the liquid helium from the pressure of the helium vapours.

The assembled cryostats can be seen in Figure 5.

Figure 5. The cryostat. The pulse solenoid is situated inside the blue foam outer cryostat. Liquid nitrogen is filled from the black plastic funnel. The white internal cryostat sits on top and the sample holder finger from the internal cryostat protrudes in to the pulse solenoid.

3.3 Thyristor discharge circuit

Energy for the magnetic field pulse is charged into a high voltage capacitor bank, which is then discharged through the pulse solenoid using the thyristor-controlled circuit with maximum discharge current of 20 kA creating the pulsed magnetic field inside the solenoid. The capacitor bank consists of two capacitors arranged into two branches of ten. Depending on the energy needed for the pulse, the branches can be used together or separately by manually modifying the connections. The discharge is triggered with a TTL (transistor-transistor logic) operation. The trigger input is fully galvanically isolated up to 10 kV. The discharge current is measured using a current probe. The circuit diagram of the thyristor discharge circuit can be seen in Figure 6, the thyristor discharger itself in Figure 7, the capacitor bank in Figure 8 and the electrical specifications of the circuit and the capacitor bank in Tables 3 and 4.

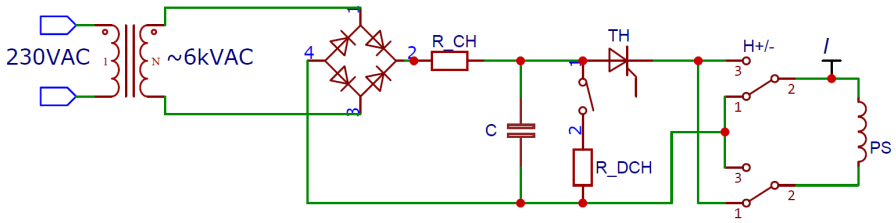

Figure 6. Circuit diagram of the discharge circuit. R_CH is the charge current limiting resistor, R_DCH is the discharge resistor for safely discharging the capacitor bank, C is the capacitor bank, TH is the discharge thyristor, H+/- is the switch for changing the polarity of the pulsed magnetic field and PS the pulse solenoid itself. I is the current probe for discharge current measurement.

Table 3. Electrical specifications of the thyristor discharge circuit.

Thyristor	4 x T630
Maximum peak current	20 kA
Working voltage range	25 V - 6 kV
Voltage rise time	200 V/μs

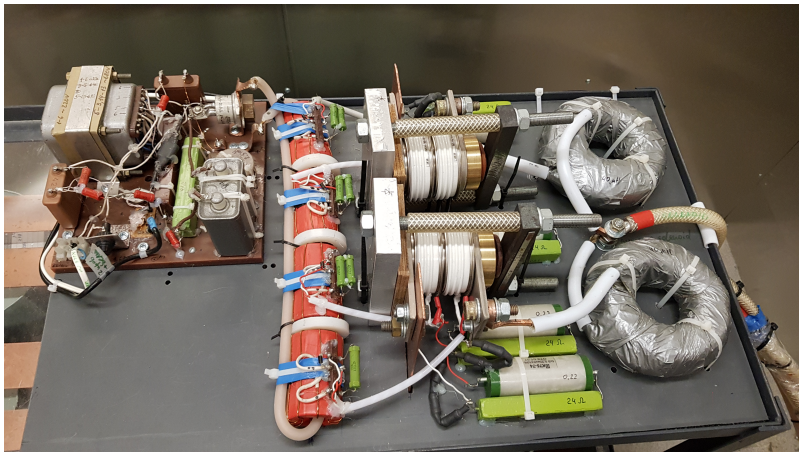

Figure 7. The thyristor discharger circuit.

Table 4. Electrical specifications of the capacitor bank.

Capacitors	20 x 2750 μF, 3.5 kV
Total capacitance	6 mF
Maximum voltage	5 kV
Maximum energy	90 kJ

Figure 8. The capacitor bank. The thyristor discharge circuit (as depicted in Figure 7) can be seen on top.

3.4 Control room

In the control room are the apparatus for controlling the PMFS and the conditions for the measurement.

The apparatus are:

- Lake Shore 332 cryogenic temperature controller
- High voltage block containing digital multimeters
- Power block
- Bias current generation (custom circuit)
- Data acquisition card
- Personal computer

Lake Shore 332 cryogenic temperature controller is for controlling the temperature of the sample immersed in the liquid helium.

The high voltage block contains 2 digital multimeters to monitor voltage on the capacitor banks and the charge current.

The power block is used to control the high voltage electronics: Turn on the control voltage, turn on the high voltage transformer to start charging the capacitor bank and start the capacitor bank discharge to the solenoid.

The bias current generator was specifically designed for the PMFS with a high output impedance to decrease noise pickup and injection into the measurement circuits. The bias current is adjustable between 5 μA and 200 mA and the polarity can be switched. By switching the current polarity possible thermal gradient voltage in the sample can be compensated. The current is supplied from AA batteries to decrease the parasitic capacitance of the current supply.

The control room apparatus can be seen in Figure 9.

Figure 9. The control room apparatus.

3.5 Measurement system

The measurement system apparatus are:

- Preamplifiers
- Base block amplifiers
- Digital-to-analog converters
- National Instruments data acquisition system

The block diagram of the measurement system can be seen in Figure 10.

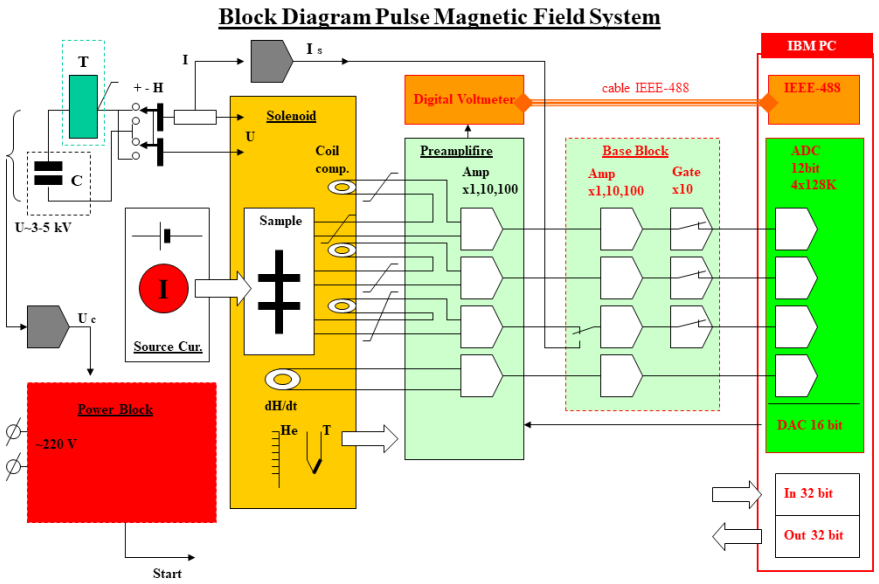

Figure 10. Block diagram of the measurement system.

The measurement system consists of two thermocouples, magnetic field sensing coil, liquid helium level meter, pulse current probe and three optional measurement channels for resistance or Hall voltage measurements. Each of the voltage measurement channels have compensation coils wound in anti-phase to the rest of the measurement loop to compensate the voltage induced from the magnetic field pulse.

The four-channel data acquisition system consists of preamplifiers, digital-to-analog converters and data-acquisition system for the personal computer in the control room. Data is captured and processed on the PC using LabView software.

The amplitude of the magnetic field pulse is measured using the sensing coil. According to Faraday's law of induction, a changing magnetic field inside the coil induces a voltage, which can be then measured using the measurement system. Because the induced voltage is proportional to the time derivative of the magnetic field, the magnetic field amplitude can be calculated by numerically integrating the measured voltage. The coil has been carefully calibrated to ensure its accuracy.

The level of liquid helium inside the cryostat is measured with a piece of superconducting wire. The wire has a critical temperature of 10 K, below which the wire becomes superconductive. Because of this, only the part of the wire submersed in the liquid helium is superconducting. Therefore the liquid helium level can be determined by measuring the

resistance of the wire.

Resistivity of the sample is measured using six terminal sensing. The bias current generated is supplied through the sample through terminals on the ends of the sample and voltage drop caused by the samples resistance is measured through terminals along the length of the sample. The Hall voltage is measured through terminals placed diagonally across the sample. The terminal configuration on a a sample can be seen in Figure 11.

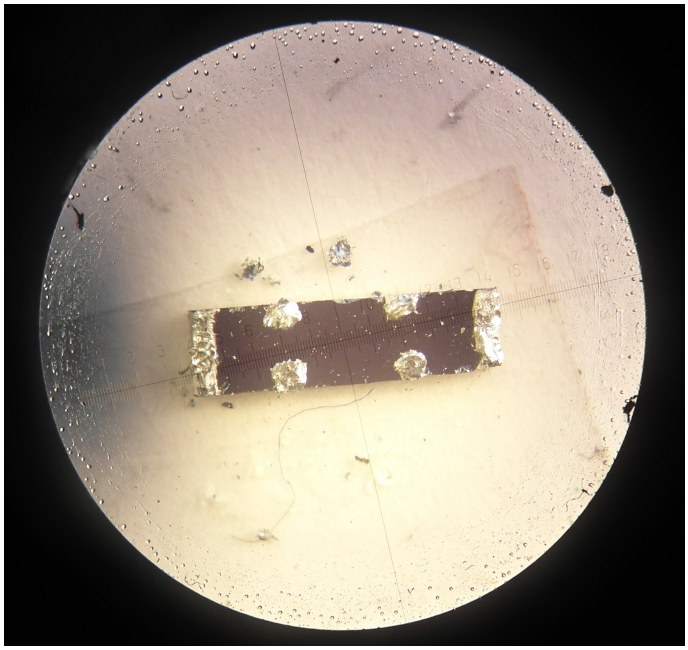

Figure 11. The measurement terminal configuration on a sample.

Inside the sample holder is a 25 W electrical heater controlled by the Lake Shore controller to heat the sample above ambient temperature if necessary. The temperature controller has low output noise to decrease the amount of noise injected into the experiment. The temperature of the sample is measured using two thermocouples; Au-Fe and Cu-Cu:Fe respectively.

The thermocouples are situated one in the body of the sample holder and one right next to the sample. Using these two thermocouples allows calculating the thermal gradient over the sample and taking it into account in the analysis of the measurement data.

The preamplifiers and base block amplifiers together amplify the signals to the correct level for the data acquisition system to ensure maximum resolution and dynamic range

and therefore minimize the noise from the analog-to-digital-conversion.

The preamplifiers convert the high impedance signals to low impedance ones to decrease the noise pickup from the transmission lines to the base block amplifier. They have a channel specific toggleable gain of 1, 10 or 100 which is selected depending on the signal levels from the sample.

The base block amplifiers are situated in the control room. They also have a toggleable gain of 1, 10 or 100 for the voltage measurement channels. It also contains a similar amplifier for the magnetic field sensing coil. If more gain for the measurement channels is necessary, there is also an additional amplifier with the gain of 10 available.

4 MEASUREMENTS

4.1 Typical samples for the PMFS

Typical samples to be used in the PMFS are experimental semiconductor materials, for example anisotropic semiconductor materials, diluted magnetic semiconductor (DMS) materials or topological structures. As a concrete example, investigation of DMS as potential materials for spintronic devices is one of the fastest growing directions of solid state physics. DMS are semiconductors with up to 10 % of ferromagnetic impurities.

Samples are usually manufactured using standard methods present in the semiconductor industry, such as different crystal growing methods, ion implantation, doping of impurities, sputtering, epitaxy and other methods of thin film deposition.

Samples can be basically any material of choice, but they are only limited by the physical size of the sample holder and the measurement range of the resistivity measurement. Also the material needs to be such, that making reliable electrical connections to it is possible. Maximum sample sizes are depicted in Figure 12.

In case of measuring thin films, the resistivity of the substrate needs to be at least 10^3 higher than that of the film for good signal-to-noise ratio.

4.2 Preparation of samples

The maximum size of the sample is defined by the sample holder, which has a semicircular cross section with a diameter of 8 mm. A wider sample has to be shorter while a narrower can be taller.

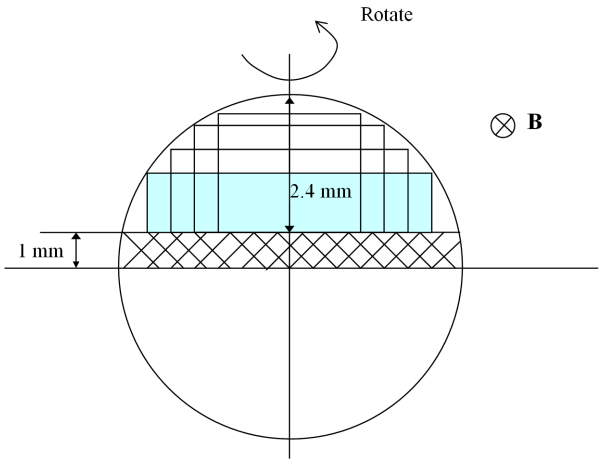

Figure 12. Maximum sizes of the sample with the direction of the magnetic field indicated.

The sample is prepared with six contacts for a six-probe measurement allowing simultaneous measurement of longitudinal and transverse voltage. Electrical connection to the sample is provided with double silk thread insulated 0.03 mm diameter copper wire, which is twisted into pairs to reduce noise and to decrease loop area to minimize the voltage induced from the magnetic field pulse. The wires are soldered to the sample using indium, because it retains its ductility and malleability in cryogenic temperature and provides a reliable low noise electrical connection [15]. Finally, the sample is fixed to the sample holder using BF-2 glue. A prepared sample not yet attached to the sample holder can be seen in Figure 13.

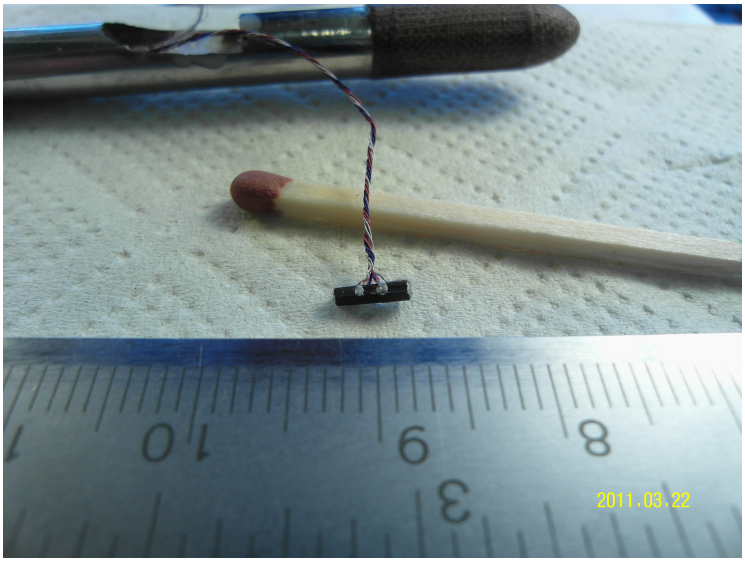

Figure 13. Prepared sample and the sample holder in the background.

The sample holder is a 11 mm outside and 8 mm inside diameter tube made of constantan (a copper-nickel alloy). The sample holder has a flat cut out for mounting the sample. The sample sits on a insulating sheet of aluminium oxide (Al_2O_3) for its good electrical insulating, non-magnetic and thermal conducting properties.

4.3 Preparation of equipment for the measurement

To prepare for the measurement, the solenoid cryostat is filled with liquid nitrogen to cool the solenoid. If necessary, the sample cryostat is filled with liquid helium.

Once the solenoid has reached temperature equilibrium, the sample in the sample holder is loaded into the cryostat. The sample connections are attached to the measurement system and then checked.

Next, the bias current for the resistivity measurement is adjusted to proper level for best signal-to-noise ratio. Once the bias current is set, the measurement system amplifier gains are set for best resolution and signal-to-noise ratio.

4.4 The measurement

The first variable to be measured is the temperature dependence of the resistivity. This can be done passively by letting the sample cryostat temperature slowly drop by heat leakage to the liquid nitrogen temperature solenoid cryostat and recording the data. If this temperature is not low enough, liquid helium is added to the sample cryostat and the temperature is controlled with the Lake Shore temperature controller.

Next, the the magnetic field dependence of the resistivity and the Hall voltage are measured. The magnetic field amplitudes and temperatures used are determined by the sample parameters and are found in most cases by trial and error.

During the measurement, the PMFS is constantly monitored. The liquid nitrogen level of the solenoid cryostat is kept at adequate levels, the gain of the amplifiers is changed if necessary to maintain best possible resolution and signal-to-noise ratio.

The amplitude of the magnetic field used in the pulse and the used temperatures are defined by the sample and the available dynamic range in the measurement system. These values are in practise determined by trial and error, by starting from a conservative starting point.

4.5 Data analysis

The measurement software, implemented as a Virtual Instrument in LabView on the PC, automatically calculates some of the most important parameters, such as the magnetic field amplitude by integration of the voltage signal from the sensing coil and the resistivity of the sample by Ohm's law from the bias current, the voltage signal along the sample and the dimensions of the sample. The software also extracts the period and slope of SdH oscillations if such exist.

Errors in the measurement can be estimated from the measured temperature gradient across the sample, the known non-homogeneity of the magnetic field and the amplifier gain settings.

There is some numerical error correction implemented in the LabView software, the parameters of which are adjusted per measurement for best possible results.

The software combines the data from all the measurements and outputs ready plots of resistivity versus temperature, resistivity versus magnetic field and Hall voltage versus magnetic field. Example of the plots produced can be seen in Figure 14, which is the data from a single magnetic field pulse.

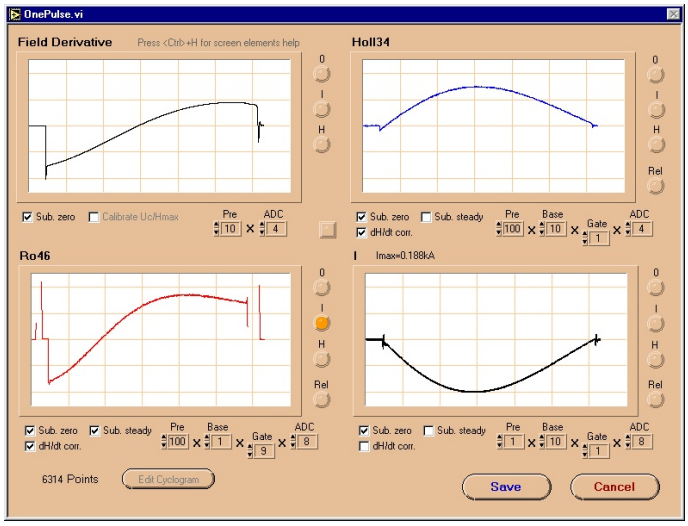

Figure 14. Example of the data captured from a single magnetic field pulse.

5 MEASUREMENT RESULTS

Using the measurements, many of the important galvanomagnetic parameters and structural characteristics of the sample can be determined.

The specific electrical conductivity of the sample is calculated using the formula

$$\sigma = \frac{I \cdot l}{V_\sigma A} \tag{5}$$

where I is the bias current through the sample, l is the distance between the sensing contacts, V_σ the voltage between the contacts and A the cross-sectional area of the sample perpendicular to the current.

The Hall constant, charge carrier charge and mobility can be calculated with the acquired data by using the formulas described in the section 2.1 and some initial knowledge of the composition of the material.

The effective mass of the charge carriers, the minority and majority carrier population identification and the shape of the materials Fermi surface can be determined by using the parameters of the SdH oscillations from the data, as described in section 2.4.

For more detailed view into the calculations of these transport parameters from measurement results see [16].

Example data from a complete set of measurements is depicted in Figure 15.

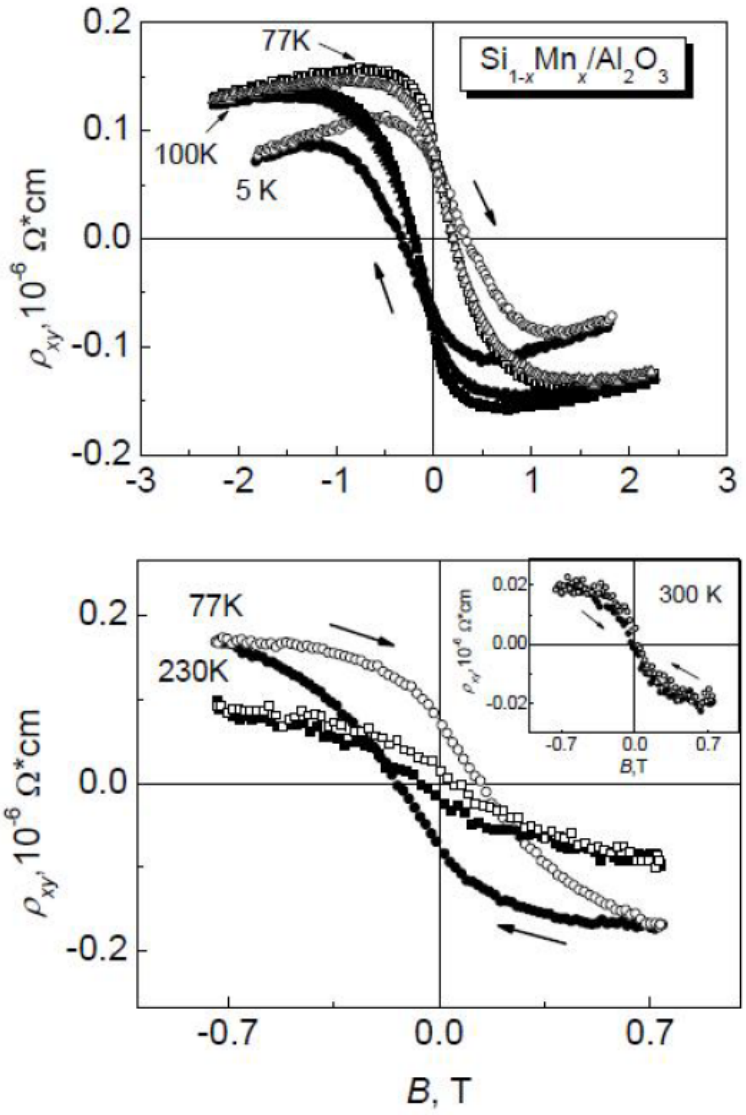

Figure 15. Example of the data from a complete set of measurements: The dependence of the longitudinal resistance as a function of magnetic field strength at different temperatures [17].

In further research this data can be used, for example, to determine the effects of specific topological structures, different doping concentrations and materials or different manufacturing methods to create new materials or structures with some specific designed characteristics. One example is developing materials with large magnetoresistance in room temperature for use as magnetic field sensors.

6 CONCLUSIONS

As introduced in this thesis, the pulsed magnetic field system (PMFS) is a versatile instrument for measurement of the temperature and magnetic field dependence of resistivity and Hall voltage in a sample. These measurements allow the determination of many transport parameters of the material under test and can provide crucial information for fundamental research of condensed matter physics, in addition to the development of new semiconductor materials as well as exploring materials for emerging technologies such as spintronics and quantum computing.

REFERENCES

[1] L Liu, Z Liu, L Huang, Z Sun, T Ma, S Zhu, X Quan, Y Yang, L Huang, and Z Luo. Pulsed magnetic field promotes proliferation and neurotrophic genes expression in schwann cells in vitro. *International journal of clinical and experimental pathology*, 8(3):2343–2353, 2015.

[2] G.V. Stephanov, V.V. Kharchenko, A.A. Kotlyarenko, and A.I. Babutskii. Effect of pulsed magnetic field treatment on the fracture resistance of a cracked specimen. *Strength of Materials*, 45(2):154–162, 2013.

[3] Edwin H. Hall. On a new action of the magnet on electric currents. *American Journal of Mathematics*, 2(3):287–292, 1879.

[4] Hugh D. Young and Roger A. Freedman. *Sears & Zemansky's University Physics with Modern Physics*, page 888. Addison-Wesley, 13th edition, 2012.

[5] Hall Effect Sensor, Electronics Tutorials. https://www.electronics-tutorials.ws/electromagnetism/hall-effect.html, 2018. [Online; accessed January, 18, 2019].

[6] R.P. Feynman, R.B. Leighton, and M. Sands. *The Feynman Lectures on Physics, Vol. III: The New Millennium Edition: Quantum Mechanics*. Basic Books, 2015.

[7] Edwin H. Hall. On the "rotational coefficient" in nickel and cobalt. *The London, Edinburgh, and Dublin Philosophical Magazine and Journal of Science*, 12(74):157–172, 1881.

[8] Emerson M Pugh. Hall effect and the magnetic properties of some ferromagnetic materials. *Physical Review*, 36(9):1503–1511, 1930.

[9] Rhys A. Griffiths. *Anomalous Hall effect measurements of bilayer magnetic structures*. PhD thesis, University of Manchester, United Kingdom, 2016.

[10] Roman Kochetov. Investigations of GaAs based heterostructures for spintronics. Master's thesis, Lappeenranta University of Technology, Finland, 2007.

[11] C. L. Chien, John Q. Xiao, and J. Samuel Jiang. Giant negative magnetoresistance in granular ferromagnetic systems (invited). *Journal of Applied Physics*, 73(10):5309–5314, 1993.

[12] J. M. Ziman. *Principles of the Theory of Solids*. Cambridge University Press, 2 edition, 1972.

[13] Shubnikov de-Haas Oscillations. http://groups.physics.umn.edu/zudovlab/content/sdho.htm. [Online; accessed January, 22, 2019].

[14] P.T. Coleridge, M. Hayne, P. Zawadzki, and A.S. Sachrajda. Effective masses in high-mobility 2d electron gas structures. *Surface Science*, 361/362:560–563, 1996.

[15] Indium solder and sealing products are successfully used in cryogenic & fusing applications by Indium Corporation. https://www.indium.com/metals/indium/indium-solder-and-sealing/. [Online; accessed January, 23, 2019].

[16] Alexander Lashkul. *Quantum transport phenomena and shallow impurity states in CdSb*. PhD thesis, Lappeenranta University of Technology, Finland, 2007.

[17] Yulia Grebenyuk. Galvanomagnetic effects in InGaAs nanostructures. Master's thesis, Lappeenranta University of Technology, Finland, 2013.